Intravascular Image-guided Coronary Artery Calcification Treatment Strategy

Kuan-Jung Hou[1,2], Ming-Yun Ho[1,2]

[1]*Division of Cardiology, Chang Gung Memorial Hospital, Linkou Medical Center, Taoyuan City, Taiwan*
[2]*School of Medicine, College of Medicine, Chang Gung University, Taoyuan City, Taiwan*

Abstract

Purpose: Coronary artery calcification (CAC) poses significant challenges in percutaneous coronary intervention (PCI), impairing device delivery, limiting stent expansion, and worsening long-term outcomes. This review summarizes current evidence on intravascular imaging (IVI)-guided assessment and treatment of calcified coronary lesions, with the aim of providing a practical framework for clinical decision-making.

Methods: We comprehensively reviewed current literature on IVI-based calcium characterization, calcified nodule (CN) identification, and image-guided lesion preparation strategies, incorporating evidence from intravascular ultrasound (IVUS) and optical coherence tomography (OCT) studies, as well as atherectomy and calcium modification trials.

Results: IVUS and OCT offer complementary assessments of calcium arc, length, depth and thickness, each with distinct advantages. Minimum calcium thickness is the key determinant of calcium fracture susceptibility, with thresholds differing before and after atherectomy. CNs represent an advanced calcification morphology associated with adverse outcomes; eruptive and non-eruptive subtypes differ in deformability and prognosis. For circumferential calcium, calcium fracture achieved through lesion preparation predicts better stent expansion. For CNs, intravascular lithotripsy is a safe escalation option, with atherectomy reserved for selected cases. In IVI-guided rotational atherectomy, wire bias assessment is critical, both to determine the debulking site and to identify high-risk vessel segments.

Conclusions: IVI is a cornerstone of calcified lesion management in contemporary PCI. Taken together, accurate morphology recognition, informed device selection, and real-time procedural guidance enabled by IVI can optimize outcomes in this challenging lesion subset.

Keywords: coronary artery calcification, intravascular imaging, intravascular ultrasound, optical coherence tomography, calcified nodule, calcium modification

How to Evaluate Calcium by OCT and IVUS

Coronary artery calcification (CAC) remains one of the most persistent challenges in percutaneous coronary intervention (PCI), even after decades of device and technique development. Device delivery is often impeded,

Received: May 31, 2026; Accepted: Jul. 5, 2026
Address for correspondence: Ming-Yun Ho, MD
Division of Cardiology, Chang Gung Memorial Hospital, Linkou Medical Center; No. 5, Fuxing St., Guishan Dist., Taoyuan City 333, Taiwan
Tel: +886-3-328-1200; E-mail: B9005017@hotmail.com

adequate stent expansion is frequently not achieved, and rotational atherectomy (RA) — when required — carries an elevated risk of vessel complications[1]. Beyond procedural difficulties, CAC worsens long-term outcomes. In a pooled analysis of 6,296 patients, severe CAC independently predicted all-cause mortality (10.8% vs. 4.4%) and the composite of death or myocardial infarction (22.9% vs. 10.9%) at three years[2]. Accurate characterization of calcification is therefore indispensable — and this is where coronary angiography falls short.

Intravascular imaging (IVI) allows more precise assessment of coronary calcification than angiography alone. Among lesions with a calcium arc ≥270°, approximately 16-30% remain undetected by angiography[3]. In current clinical practice, intravascular ultrasound (IVUS) and optical coherence tomography (OCT) are the primary modalities for intravascular calcium assessment, with each offering unique capabilities. Both IVUS and OCT evaluate calcium arc, depth and length. Beyond arc and length, OCT also measures calcium thickness[4] and enables more detailed characterization of calcified nodules[5,6] (Figures 1A and 1B, Table 1).

From a pathohistological perspective, coronary calcification is classified into six morphological types: microcalcification (≥0.5 μm to <15 μm), punctate calcification (>15 μm to <1 mm), fragment calcification (≥1 mm), sheet calcification (involving more than one

Table 1. Comparison between IVUS and OCT for calcification assessment

Calcium parameter	IVUS	OCT
Calcium arc	Adequate	Adequate
Calcium depth	Superior (deeper layer)	Adequate
Calcium length	Adequate	Superior
Calcium thickness	Cannot penetrate calcium	Superior
Calcified nodules	Adequate	Superior

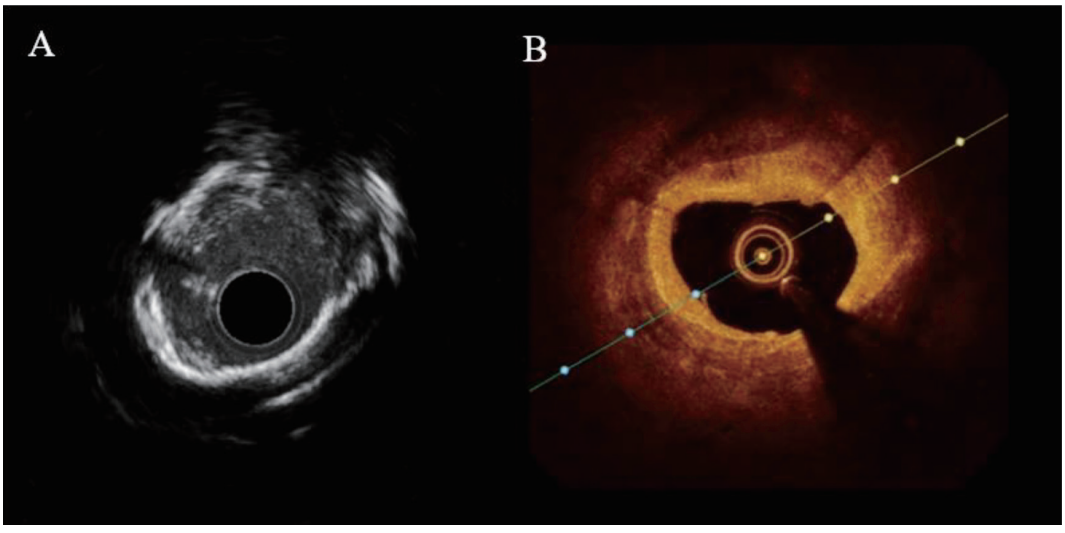

Figure 1. Representative intravascular images of coronary calcification. **(A)** IVUS image showing a hyperechoic leading edge with posterior acoustic shadowing. **(B)** OCT image showing a signal-poor region with sharply delineated borders, allowing measurement of calcium arc and thickness.

quadrant of the vessel circumference), nodular calcification (nodular deposits confined to the plaque without luminal disruption), and calcified nodule (fragmented calcium protruding into the lumen, typically associated with overlying thrombus). This spectrum represents a cumulative progression, ultimately leading to ossification in advanced cases[7]. The more advanced the morphology seen on imaging, the greater the underlying lesion burden.

CAC assessment by IVI primarily covers three key dimensions: calcium length, arc and depth. Calcium length refers to the extent of continuous calcification along the longitudinal axis of the vessel. Calcium arc is the central angle of calcium involvement at a single cross-section, measured in degrees. Calcium depth is classified as superficial when the calcium leading edge lies within the inner 50% of the combined plaque and media thickness, and otherwise as deep[3,4].

On OCT imaging, calcification is identified as a signal-poor region with a sharply delineated border[6]. OCT allows measurement of calcium thickness; however, its application of near-infrared light limits penetration depth to, at most, 1.0 mm in the absence of lipid interference, with this limit reduced to approximately 0.63 mm when lipid is present[6,8] (Figure 2). In addition to this technical limitation, lipid pools and calcification share a similar low-signal appearance, and therefore careful differentiation between the two is required. Calcification with greater thickness typically exhibits structural continuity; on longitudinal assessment, well-defined borders remain visible in segments proximal and distal to the most severely calcified region, in contrast to the poorly defined or diffuse borders of lipid pools[9].

On IVUS imaging, calcification is identified by its hyperechoic leading edge with posterior acoustic shadowing[3]. IVUS is highly sensitive for calcium detection and allows assessment of calcium arc and length. However, calcium thickness cannot be directly assessed by IVUS, as acoustic shadowing obscures the calcium trailing edge[3]. To overcome this limitation, several indirect approaches can allow an estimation of calcium thickness. First, calcium thickness can be approximated from the vessel diameter at the non-calcified arc and the extent of acoustic shadowing within the same cross-section, under the premise of a circular cross-section (Figures 3A and 3B). Second, when 60-MHz IVUS shows impermeable acoustic shadowing, calcium thickness is most likely greater than 0.5 mm[10] (Figures 4A and 4B). Third, among lesions with reverberation on IVUS, 54.6% have a calcium thickness less than 0.5 mm, as determined by OCT[3]. A retrospective study showed that more reverberation layers indicate thicker calcification: single-, double- and multi-layer reverberation correspond to median calcium thicknesses of 0.62 mm, 0.95 mm and 1.18 mm, respectively[11].

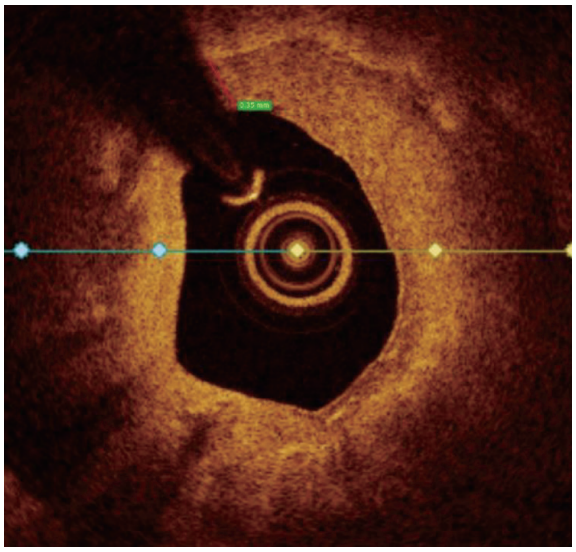

Figure 2. OCT image of a superficially calcified plaque with a signal-poor region and sharply delineated border. Calcium thickness was measured at 0.35 mm, demonstrating OCT's capability for direct thickness quantification.

IVUS and OCT are complementary modalities, enabling assessment of calcium arc, length, depth and thickness. These parameters are critical for treatment planning and strategy optimization in calcified lesions.

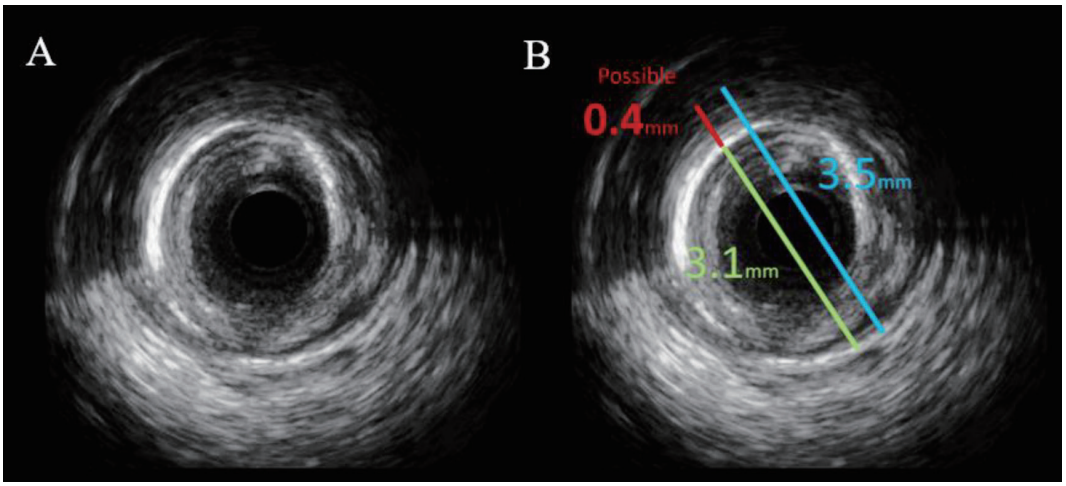

Figure 3. Indirect estimation of calcium thickness by IVUS. **(A)** IVUS image showing a hyperechoic leading edge with posterior acoustic shadowing, precluding visualization of the calcium trailing edge and direct thickness measurement. **(B)** Calcium thickness can be estimated by comparing the vessel diameter at the non-calcified arc (3.5 mm, blue) with the diameter at the calcified arc (3.1 mm, green), yielding an estimated calcium thickness of 0.4 mm (red).

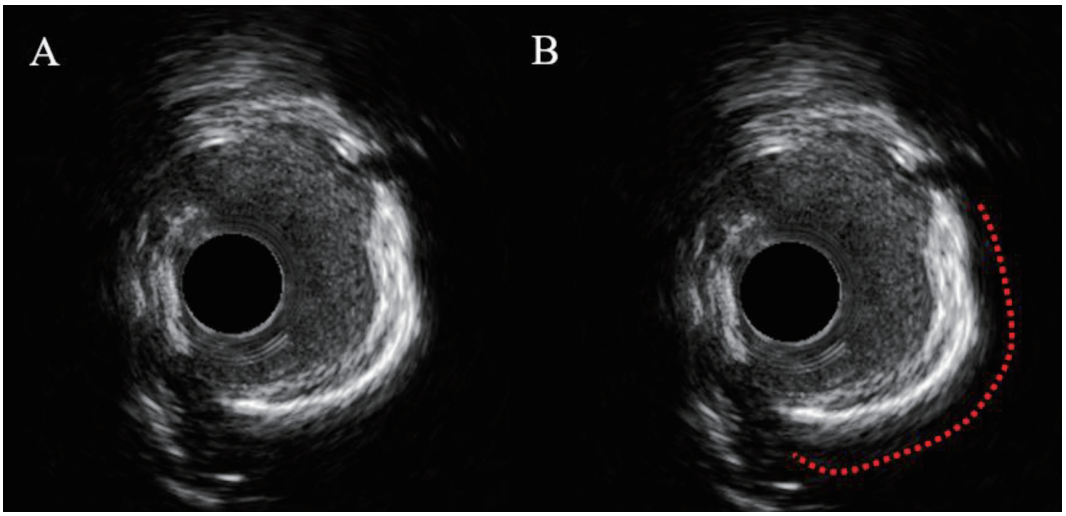

Figure 4. IVUS assessment of calcium permeability. **(A)** IVUS image showing a calcified lesion. **(B)** Impermeable acoustic shadowing (red dotted line) on 60-MHz IVUS, suggesting a calcium thickness likely greater than 0.5 mm.

Unlocking the Mystery of Calcified Nodules

Calcified nodules (CNs) are a specific type of heavily calcified coronary lesion characterized by luminal protrusion of calcium, representing an advanced and severe stage of coronary calcification and carrying an increased risk of adverse clinical outcomes[7,12,13]. While this protruding calcification retains relative structural integrity, it may progress into classic CNs characterized by fragmented calcium protruding into the lumen, in either eruptive or non-eruptive form[12,13].

On OCT imaging, CNs appear as highly backscattering luminal protrusions with signal attenuation, an appearance that closely resembles red thrombus[6,14,15]. Several mechanisms may account for this pattern. First, intraplaque hemorrhage or an adherent thrombus on the nodule surface attenuates the signal[6,8,13,16]. Second, a sufficiently thick calcium layer makes the trailing edge invisible[6]. Last, a necrotic core within the CN impairs OCT penetration[8,13]. The shared signal attenuation pattern of CNs and red thrombus makes their differentiation essential. CNs typically show structural continuity with sheet or fragment calcification extending into adjacent vessel segments, whereas red thrombus lacks this continuity[12,13,15] (Figures 5A and 5B).

CNs are more commonly found in coronary arteries with higher calcium burden and at segments with greater vessel angulation. Mid left anterior descending artery (LAD) and mid right coronary artery (RCA) account for the highest number of CN lesions, with a noted predilection for the ostial and mid RCA. This distribution suggests that mechanical stress and vessel angulation contribute to CN formation[17].

Regarding treatment response, eruptive CNs are highly deformable, with 100% deformability reported in an intravascular lithotripsy (IVL) pooled analysis, compared with approximately two-thirds of non-eruptive CNs[18]. This significant difference stems from the more compliant structure of eruptive CNs, comprising the lack of collagen matrix, intraplaque hemorrhage, small calcium fragments, and necrotic core calcification[12,13]. These features render eruptive CNs more expandable.

Despite better stent expansion, eruptive CNs are paradoxically associated with worse clinical outcomes after PCI. The 2-year target lesion revascularization (TLR) rate was significantly higher in eruptive CNs compared with non-eruptive CNs (18.3% vs. 9.6%; P=0.04)[19]. Given the complexity of imaging interpretation and intervention planning, the optimal treatment strategy for CNs remains open for debate, warranting further research.

How to use Image Guidance to Treat Calcium

The application of IVI to guide the treatment of calcified lesions is of great importance.

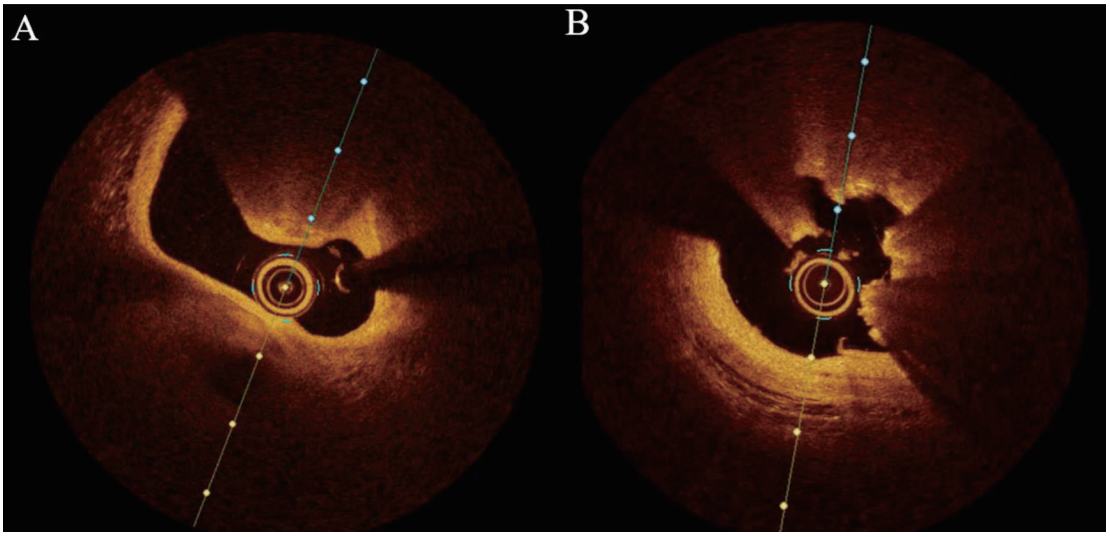

Figure 5. OCT images of calcified nodules. **(A)** Non-eruptive calcified nodule with a smooth intact fibrous cap. **(B)** Eruptive calcified nodule showing fragmented calcium disrupting the overlying fibrous cap and protruding into the lumen.

Circumferential calcium and CNs are the two morphologies most frequently associated with stent under-expansion and target lesion revascularization[1,12] (Figures 6A and 6B). Identification of these two morphologies by IVI is therefore essential to determine the appropriate treatment strategy.

Two OCT-derived thresholds have been identified as predictors of calcium fracture created by balloon angioplasty alone: a maximum calcium arc greater than 225° and a minimum calcium thickness less than 0.24 mm[20]. The balloon applies symmetric pressure at both edges of the calcified ring, forcing fracture at the thinnest point. The presence of a "weak point" is therefore the key determinant of whether balloon angioplasty alone can create fracture.

In 2018, Fujino et al. developed the first OCT-based calcium scoring system to predict stent under-expansion. The score incorporated three parameters: maximum calcium arc, maximum calcium thickness, and calcium length. However, the study was skewed towards lesions of low-to-intermediate complexity. Furthermore, thickness was measured at its maximum rather than minimum value[21]. The thickest point is less susceptible to fracture, thus limiting the clinical applicability of this scoring system.

Sato et al. addressed this limitation by replacing maximum with minimum calcium thickness in a revised scoring system, restricted to lesions with a maximum calcium arc exceeding 270°[22]. This revised scoring system assigns one point to each of three criteria: a minimum calcium thickness greater than 0.3 mm, circumferential (360°) calcium, and a calcium arc greater than 270° with a length longer than 3 mm. Calcium fracture rates fell with increasing minimum calcium thickness — 71% for less than 0.3 mm, 54% for 0.3 to 0.49 mm, and 17% for 0.5 mm or greater[22]. Minimum calcium thickness thus emerges as the key determinant of susceptibility to calcium fracture[22], with the site of minimum calcium thickness taken as the target of calcium modification.

Among calcium-modification procedures, atherectomy, such as rotational atherectomy (RA), reduces calcium volume and alters calcification structure, in turn increasing balloon-calcium contact area and improving balloon dilatation (Figures 7A and 7B). Following RA, balloon angioplasty achieves calcium fracture in lesions with a calcium arc exceeding 227° and a minimum thickness of up to 0.67 mm[23] — greater than the 0.5 mm limit reported for balloon angioplasty alone[22]. Orbital atherectomy facilitates calcium fracture at modified sites, where fracture thickness can reach up to 0.58 mm, compared with 0.45 mm at unmodified sites[24]. In lesions treated with RA followed by cutting balloon angioplasty,

Figure 6. Schematic illustrations of the two calcification morphologies most frequently associated with stent under-expansion. **(A)** Circumferential calcium. **(B)** Calcified nodule with luminal protrusion.

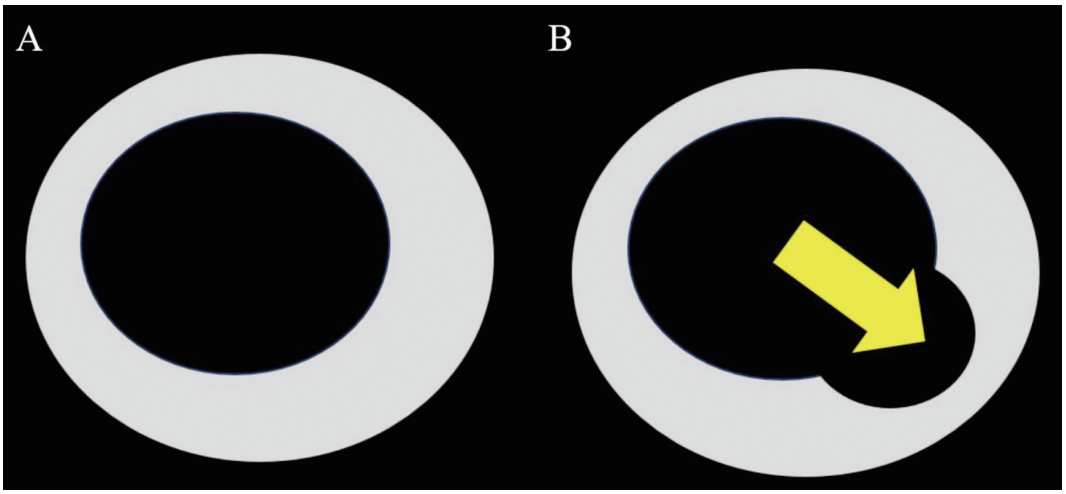

Figure 7. Effect of atherectomy on balloon-calcium contact. **(A)** Before atherectomy, circumferential calcium limits direct balloon-calcium contact. **(B)** After atherectomy, partial calcium ablation (yellow arrow) increases balloon-calcium contact area, thereby enhancing the efficacy of subsequent balloon dilatation.

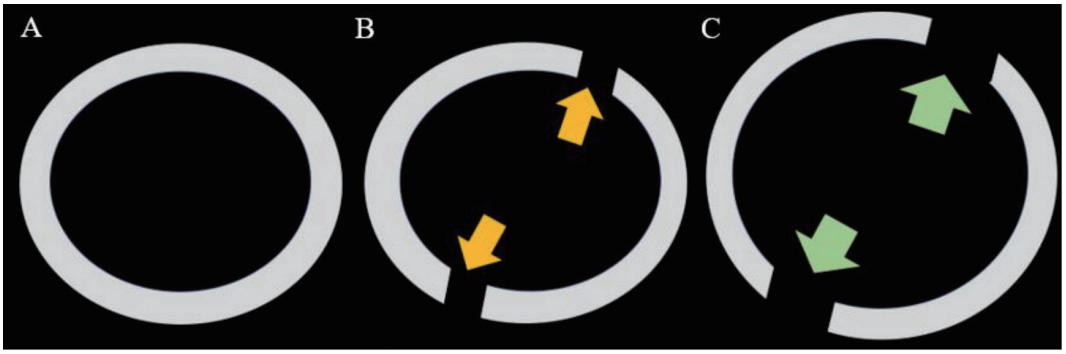

Figure 8. Relationship between calcium fracture and stent expansion. **(A)** Intact circumferential calcium without fracture. **(B)** Calcium fracture (orange arrows) enabling luminal expansion. **(C)** Multiple calcium fractures (green arrows), associated with better stent expansion.

fracture thickness is greater at modified sites than at unmodified sites (0.87 mm vs. 0.65 mm)[25]. Together, these study results confirm that debulking enhances the efficacy of subsequent balloon-based devices.

The achievement of calcium fracture predicts better stent expansion, and the greater the number of fractures, the better the stent expansion[25,26] (Figures 8A-8C). Therefore, an assessment of the presence and number of calcium fractures by intravascular imaging can tell the operator how well the lesion has been prepared in the case of circumferential calcium (Figures 9A-9D).

Intravascular lithotripsy (IVL) is another method of calcium modification. IVL delivers pulsatile acoustic pressure waves that create microfractures in both superficial and deep calcium. In the Disrupt CAD III OCT sub-study, IVL produced multiplanar and longitudinal calcium fractures in 67.4% of lesions and facilitated stent implantation despite severe calcification, with favorable stent expansion regardless of whether fractures were visible on OCT[27]. This benefit came with a favorable safety profile, as no patient developed no-reflow and no perforation occurred after IVL before stenting[27].

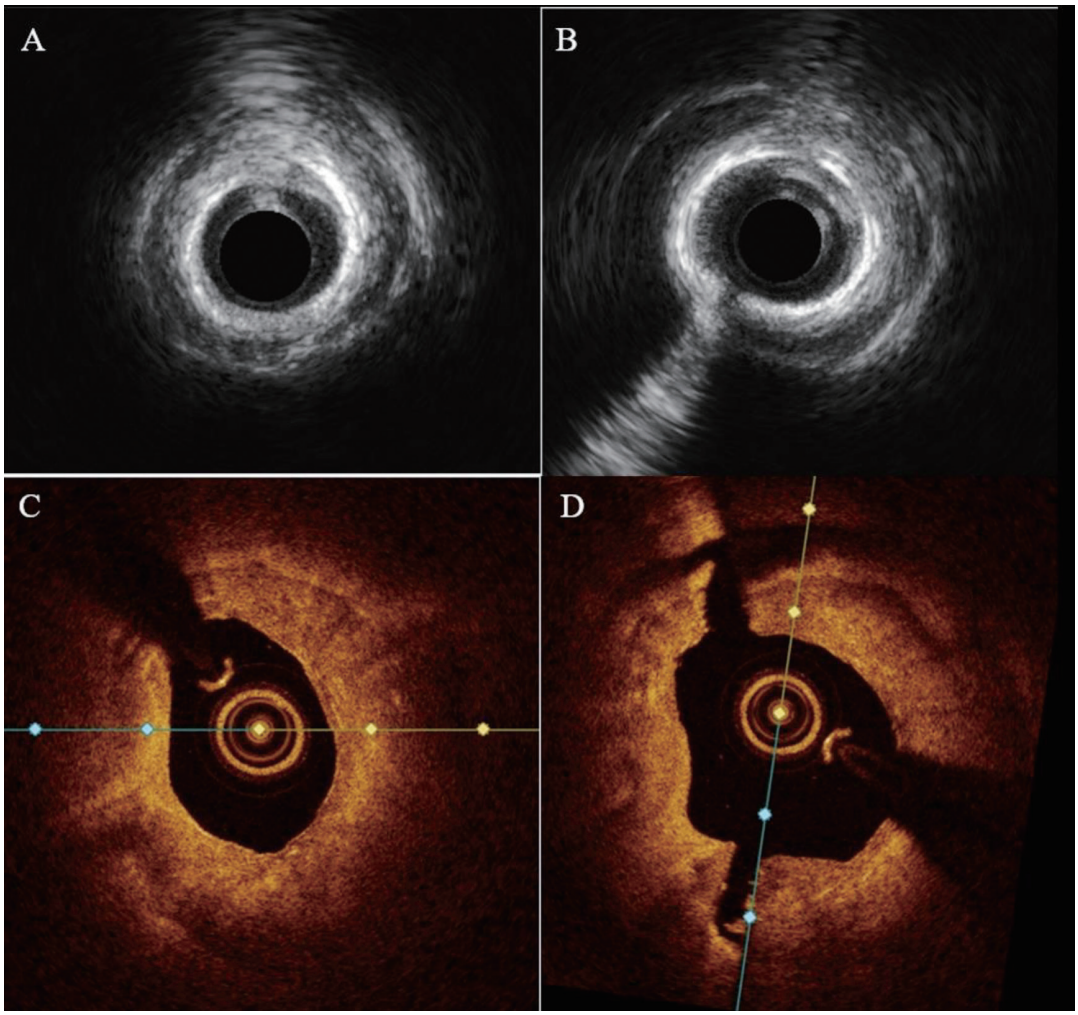

Figure 9. Calcium fracture assessment by IVUS and OCT before and after intervention. **(A, B)** IVUS images before and after calcium modification, demonstrating interruption of acoustic shadowing at the fracture site. **(C, D)** OCT images before and after calcium modification, demonstrating discontinuity of the calcified border at the fracture site.

However, the IVL balloon may fail to cross a tight, severely calcified lesion. In this situation, atherectomy can first create a pilot channel to enable IVL delivery — a combined approach termed "RotaTripsy" for RA and "Orbital-Tripsy" for OA.[28] In a RotaTripsy case series, RA modified the intimal calcium while subsequent IVL fractured the deeper calcium, and intravascular imaging revealed both IVL-induced deep fractures and RA-induced intimal microdissections[29].

By contrast, the treatment of CNs is more complex. Luminal expansion in the setting of CNs can be accomplished by direct compression of the nodule due to its deformable structure, debulking by atherectomy to increase luminal area, or fracture of the surrounding calcification to indirectly improve overall vessel compliance (Figure 10). For eruptive CNs, balloon angioplasty is seen as initial lesion preparation owing to its relative deformability. If full balloon expansion can be achieved, direct stent deployment is feasible. Otherwise, IVL is a reasonable escalation option given its favorable safety profile; atherectomy is generally not required unless upfront debulking is

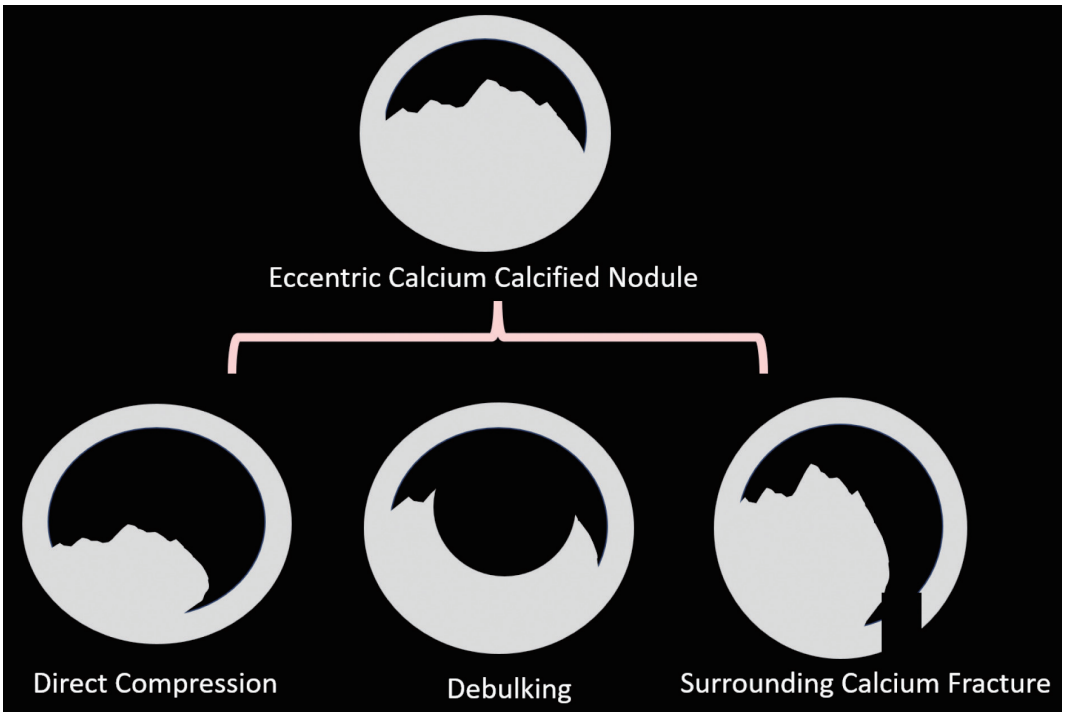

Figure 10. Three mechanisms of luminal expansion in the treatment of calcified nodules: direct compression of the deformable nodule, debulking by atherectomy, and fracture of the surrounding calcification.

needed to facilitate equipment delivery[12].

Full balloon expansion should be confirmed in two orthogonal views before proceeding to advanced lesion preparation[12]. When calcium modification is indicated, the minimum lumen diameter at the CN site can help guide device selection; a value below 1.5 mm favors atherectomy over IVL[30]. Although atherectomy facilitates equipment delivery, it has not been shown to reduce ischemia-driven target vessel revascularization (TVR) in lesions with CNs[31]. Additionally, the ARCADIA technique, in which a guidewire is advanced through the CN core, has been reported as a potential option for eccentric CNs[32].

In summary, IVI-guided treatment of calcified lesions requires accurate recognition of the morphology and a tailored strategy. In the case of circumferential calcium, the calcium arc, length and minimum thickness together predict calcium fracture and guide device selection; lesions with greater calcium thickness or length may require advanced lesion preparation. In the case of CNs, while multiple treatment strategies have been investigated, the optimal approach should be customized to individual lesion characteristics and clinical scenarios. Of note, even after adequate expansion, CNs remain associated with a higher long-term cardiovascular risk, making them one of the most challenging lesions in contemporary PCI[12,19].

Image-guided Atherectomy

In addition to lesion preparation, IVI plays an important role in pre-procedural assessment and strategic planning for RA. Although RA does not improve long-term clinical outcomes in calcified lesions, approximately 12.5% of lesions still require RA due to failure of device delivery or suboptimal balloon expansion despite non-compliant balloon use[33]. RA ablates calcified plaque, thereby enhancing the efficacy of subsequent balloon dilatation. Of note, lesion

preparation with a small burr is sufficient to facilitate device delivery and balloon expansion in most cases[33]. IVI guidance is therefore important to balance safety and efficacy during RA.

IVI can also predict the site of RA and the debulking course before the procedure. Studies show that when the imaging catheter and the guidewire are located within the same quadrant on pre-RA imaging, the debulked region is distributed within the same quadrant in 96% of cross-sections; when the two are separated, the actual debulking route may deviate from what imaging predicted[34,35]. As a short monorail system, the imaging catheter may not track the guidewire during advancement, deviating from the guidewire path and consequently from the actual debulking site (Figures 11A and 11B).

IVI also enables assessment of the contact force exerted by the imaging catheter against the vessel wall. As the imaging catheter is advanced along the targeted ablation area, wire bias may cause the catheter to push against the vessel wall — a phenomenon termed the tenting effect, which manifests as an increase in contact angle. A larger contact angle reflects greater wire bias, which directs the burr toward the calcified plaque, thereby enhancing the ablation effect. However, when the tenting effect occurs in a normal vessel segment, it may distort the vessel structure and pose a higher risk of vessel injury[36]. Kawaguchi et al. demonstrated a significant association between vessel distortion and coronary perivascular trauma[37]. Lee et al. identified two OCT predictors of vessel injury during atherectomy: a contact angle greater than 92° and a contact length greater than 0.8 mm[38]. In this way, IVI allows operators to recognize high-risk debulking areas and avoid vessel complications during atherectomy (Figures 12A and 12B).

In summary, wire bias is a key determinant in IVI-guided RA assessment, especially regarding procedural safety. While ablation effect can be estimated from IVI, treatment outcomes are influenced by multiple factors, including operator technique, rotational speed, and device selection. The primary value of IVI therefore lies in the recognition of high-risk debulking areas, enabling operators to reduce the risk of vessel rupture. For high-risk lesions, halfway RA may be considered, performing RA in the safer portion while saving balloon dilatation for the high-risk portion[39].

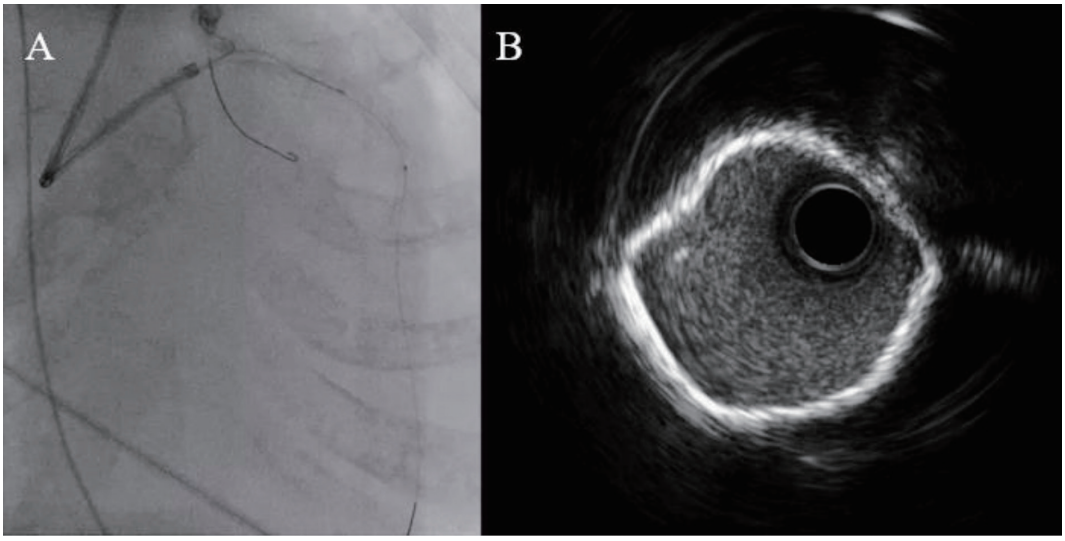

Figure 11. Prediction of the rotational atherectomy debulking site by intravascular imaging. **(A)** Fluoroscopic image demonstrating the guidewire course. **(B)** IVUS image showing separation of the imaging catheter from the guidewire, suggesting a possible deviation from the image prediction.

Conclusion

The role of IVI in calcified lesion management can be summarized in terms of device selection and procedural optimization. Without prior atherectomy, a minimum calcium thickness greater than 0.5 mm generally requires advanced lesion preparation, including the use of a non-compliant balloon, RA or IVL, to achieve calcium fracture[22]. After atherectomy combined with cutting balloon or IVL, effective calcium modification can be achieved even when minimum calcium thickness exceeds 0.8 mm, enabling better device delivery and stent expansion[25]. For more severe lesions, a larger burr or high-speed orbital atherectomy, combined with non-compliant balloon or IVL, may be considered to improve vessel compliance. This image-guided assessment framework integrates calcium arc and minimum thickness to guide device selection before and after atherectomy (Figure 13).

For borderline lesions, calcium length is an additional determinant aside from thickness; longer calcified segments often require more

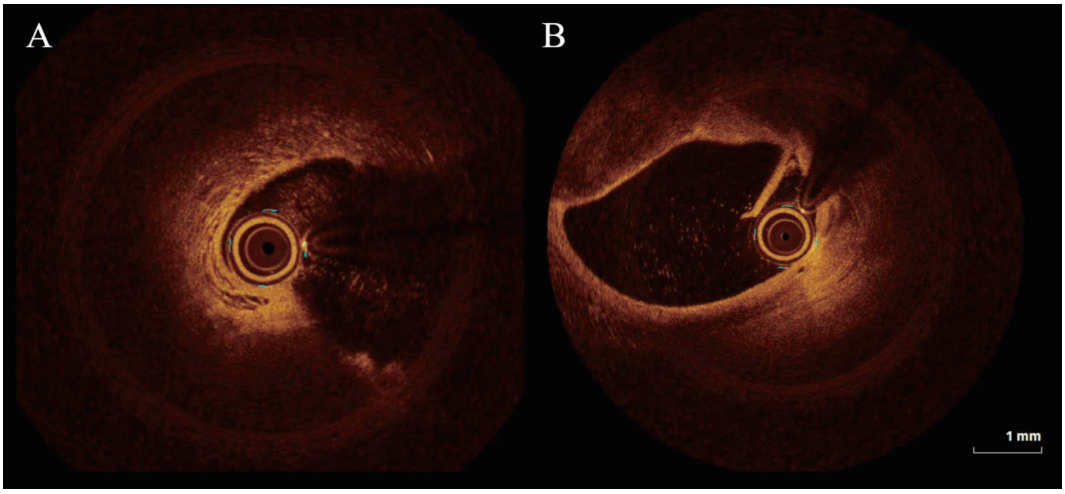

Figure 12. OCT images of vessel injury during rotational atherectomy. **(A)** Vessel perforation. **(B)** Vessel dissection.

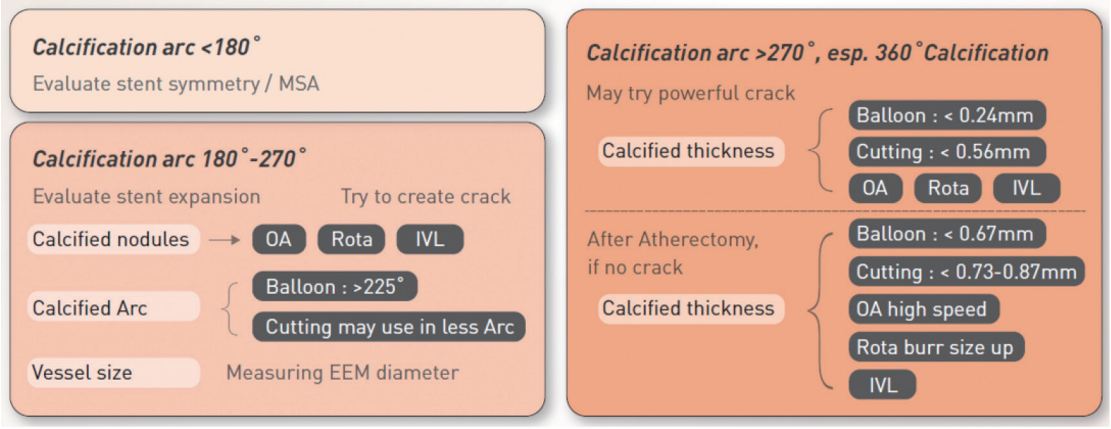

Figure 13. Image-guided treatment strategy for calcified lesions based on calcium arc and minimum calcium thickness, with device selection before and after atherectomy. This figure summarizes the conclusions of several published studies[20,23,25,40,41].

aggressive or multi-device strategies to achieve adequate lesion preparation[22]. For CNs, although the optimal treatment strategy is yet to be defined, IVL is considered a relatively safe and feasible option[12]. If acceptable wire bias is confirmed on IVI, atherectomy may be considered for upfront debulking to reduce calcium burden and optimize treatment outcomes[38].

Overall, IVI not only guides the selection of treatment strategy, but also offers real-time risk assessment, allowing timely procedural adjustment throughout the intervention. IVI is therefore a cornerstone of calcified lesion management in contemporary PCI.

List of Abbreviations

CAC: coronary artery calcification
CN: calcified nodule
IVI: intravascular imaging
IVL: intravascular lithotripsy
IVUS: intravascular ultrasound
LAD: left anterior descending artery (LAD)
OCT: optical coherence tomography
PCI: percutaneous coronary intervention
RA: rotational atherectomy
RCA: right coronary artery
TLR: target lesion revascularization
TVR: target vessel revascularization

References

1. Madhavan MV, Tarigopula M, Mintz GS, Maehara A, Stone GW, Genereux P. Coronary artery calcification: pathogenesis and prognostic implications. *J Am Coll Cardiol* 2014;63(17):1703-14.
2. Bourantas CV, Zhang YJ, Garg S, et al. Prognostic implications of coronary calcification in patients with obstructive coronary artery disease treated by percutaneous coronary intervention: a patient-level pooled analysis of 7 contemporary stent trials. *Heart* 2014;100(15): 1158-64.
3. Wang X, Matsumura M, Mintz GS, et al. In Vivo Calcium Detection by Comparing Optical Coherence Tomography, Intravascular Ultrasound, and Angiography. *JACC Cardiovasc Imaging* 2017; 10(8):869-79.
4. Kume T, Okura H, Kawamoto T, et al. Assessment of the coronary calcification by optical coherence tomography. *EuroIntervention* 2011;6(6):768-72.
5. Mintz GS, Matsumura M, Ali Z, Maehara A. Clinical Utility of Intravascular Imaging: Past, Present, and Future. *JACC Cardiovasc Imaging* 2022;15(10):1799-820.
6. Saita T, Fujii K, Hao H, et al. Histopathological validation of optical frequency domain imaging to quantify various types of coronary calcifications. *Eur Heart J Cardiovasc Imaging* 2017;18(3):342-9.
7. Torii S, Mustapha JA, Narula J, et al. Histopathologic Characterization of Peripheral Arteries in Subjects With Abundant Risk Factors: Correlating Imaging With Pathology. *JACC Cardiovasc Imaging* 2019;12(8 Pt 1):1501-13.
8. Ijichi T, Nakazawa G, Torii S, et al. Evaluation of coronary arterial calcification - Ex-vivo assessment by optical frequency domain imaging. *Atherosclerosis* 2015;243(1):242-7.
9. Mintz GS. Intravascular imaging of coronary calcification and its clinical implications. *JACC Cardiovasc Imaging* 2015;8(4):461-71.
10. Oshikiri Y, Ishida M, Sakamoto R, et al. Evaluation of the thickness of coronary calcium by 60-MHz intravascular ultrasound: head-to-head comparison with optical frequency domain imaging. *Int J Cardiovasc Imaging* 2023;39(12):2599-607.
11. You W, Zhang HL, Xu T, et al. Preliminary study of the significance of reverberation by IVUS detection for patients with severe calcified lesions. *Int J Cardiovasc Imaging* 2023;39(3):667-76.
12. Shin D, Karimi Galougahi K, Spratt JC, et al. Calcified Nodule in Percutaneous Coronary Intervention: Therapeutic Challenges. *JACC Cardiovasc Interv* 2024;17(10):1187-99.
13. Ali ZA, Spratt JC, Finn AV, Maehara A, Shin D. Identification and treatment of calcified nodules in percutaneous coronary intervention. *EuroIntervention* 2025;21(23):e1424-e33.
14. Hao H, Fujii K, Shibuya M, et al. Different findings in a calcified nodule between histology and intravascular imaging such as intravascular ultrasound, optical coherence tomography, and coronary angioscopy. *JACC Cardiovasc Interv* 2014;7(8):937-8.
15. Fujii K, Kubo T, Otake H, et al. Expert consensus statement for quantitative measurement and morphologic assessment of optical coherence tomography: update 2025. *Cardiovasc Interv Ther* 2025;40(2):226-33.
16. Chin CY, Matsumura M, Maehara A, et al. Coronary Plaque Characteristics in Hemodialysis-Dependent Patients as Assessed by Optical Coherence

Tomography. *Am J Cardiol* 2017;119(9):1313-9.
17. Lee T, Mintz GS, Matsumura M, et al. Prevalence, Predictors, and Clinical Presentation of a Calcified Nodule as Assessed by Optical Coherence Tomography. *JACC Cardiovasc Imaging* 2017;10(8):883-91.
18. Ali ZA, Kereiakes D, Hill J, et al. Safety and Effectiveness of Coronary Intravascular Lithotripsy for Treatment of Calcified Nodules. *JACC Cardiovasc Interv* 2023;16(9):1122-4.
19. Sato T, Matsumura M, Yamamoto K, et al. Impact of Eruptive vs Noneruptive Calcified Nodule Morphology on Acute and Long-Term Outcomes After Stenting. *JACC Cardiovasc Interv* 2023;16(9):1024-35.
20. Fujino A, Mintz GS, Lee T, et al. Predictors of Calcium Fracture Derived From Balloon Angioplasty and its Effect on Stent Expansion Assessed by Optical Coherence Tomography. *JACC Cardiovasc Interv* 2018;11(10):1015-7.
21. Fujino A, Mintz GS, Matsumura M, et al. A new optical coherence tomography-based calcium scoring system to predict stent underexpansion. *EuroIntervention* 2018;13(18): e2182-e9.
22. Sato T, Matsumura M, Yamamoto K, et al. A Revised Optical Coherence Tomography-Derived Calcium Score to Predict Stent Underexpansion in Severely Calcified Lesions. *JACC Cardiovasc Interv* 2025;18(5):622-33.
23. Maejima N, Hibi K, Saka K, et al. Relationship Between Thickness of Calcium on Optical Coherence Tomography and Crack Formation After Balloon Dilatation in Calcified Plaque Requiring Rotational Atherectomy. *Circ J* 2016;80(6):1413-9.
24. Yamamoto MH, Maehara A, Kim SS, et al. Effect of orbital atherectomy in calcified coronary artery lesions as assessed by optical coherence tomography. *Catheter Cardiovasc Interv* 2019;93(7):1211-8.
25. Amemiya K, Yamamoto MH, Maehara A, et al. Effect of cutting balloon after rotational atherectomy in severely calcified coronary artery lesions as assessed by optical coherence tomography. *Catheter Cardiovasc Interv* 2019;94(7):936-44.
26. Kubo T, Shimamura K, Ino Y, et al. Superficial Calcium Fracture After PCI as Assessed by OCT. *JACC Cardiovasc Imaging* 2015;8(10):1228-9.
27. Hill JM, Kereiakes DJ, Shlofmitz RA, et al. Intravascular Lithotripsy for Treatment of Severely Calcified Coronary Artery Disease. *J Am Coll Cardiol* 2020;76(22):2635-46.
28. Wong B, Kam KK, So CY, et al. Synergistic Coronary Artery Calcium Modification With Combined Atherectomy and Intravascular Lithotripsy. *J Invasive Cardiol* 2023;35(3):E128-e35.
29. Gonzálvez-García A, Jiménez-Valero S, Galeote G, Moreno R, López de Sá E, Jurado-Román A. "RotaTripsy": Combination of Rotational Atherectomy and Intravascular Lithotripsy in Heavily Calcified Coronary Lesions: A Case Series. *Cardiovasc Revasc Med* 2022;35:179-84.
30. Yasumura K, Koshy AN, Vinayak M, et al. Rotational, orbital atherectomy and intravascular lithotripsy for coronary calcified nodules: insights from optical coherence tomography. *Catheter Cardiovasc Interv* 2024;104(7):1373-86.
31. Watanabe Y, Sakakura K, Taniguchi Y, et al. Comparison of clinical outcomes of intravascular ultrasound-calcified nodule between percutaneous coronary intervention with versus without rotational atherectomy in a propensity-score matched analysis. *PLoS One* 2020;15(11): e0241836.
32. Sudo K, Yasuda M, Yamasaki T, et al. 3-Dimensional Wiring Allows for ARCADIA Technique Followed by Rotational Atherectomy for Calcified Nodules. *JACC Case Rep* 2025;30(35):105165.
33. Abdel-Wahab M, Richardt G, Joachim Buttner H, et al. High-speed rotational atherectomy before paclitaxel-eluting stent implantation in complex calcified coronary lesions: the randomized ROTAXUS (Rotational Atherectomy Prior to Taxus Stent Treatment for Complex Native Coronary Artery Disease) trial. *JACC Cardiovasc Interv* 2013;6(1):10-9.
34. Hashimoto K, Fujii K, Shibutani H, et al. Prediction of optimal debulking segments before rotational atherectomy based on pre-procedural intravascular ultrasound findings. *Int J Cardiovasc Imaging* 2021; 37(3):803-12.
35. Hamana T, Kawamori H, Toba T, et al. Prediction of the debulking effect of rotational atherectomy using optical frequency domain imaging: a prospective study. *Cardiovasc Interv Ther* 2023;38(3):316-26.
36. Sakakura K, Ito Y, Shibata Y, et al. Clinical expert consensus document on rotational atherectomy from the Japanese association of cardiovascular intervention and therapeutics: update 2023. *Cardiovasc Interv Ther* 2023;38(2):141-62.
37. Kawaguchi Y, Tamura T, Masuda S, et al. Impact of the Degree of Wire Bias in the Vessel's Healthy Portion on Coronary Perivascular Trauma in Rotational Atherectomy. *Cardiovasc Revasc Med* 2022;40:123-31.
38. Lee T, Ashikaga T, Nozato T, et al. Predictors of coronary artery injury after orbital atherectomy as assessed by optical coherence tomography. *Int J Cardiovasc Imaging* 2023;39(7):1367-74.
39. Sakakura K, Taniguchi Y, Matsumoto M, Wada H,

Momomura S, Fujita H. How Should We Perform Rotational Atherectomy to an Angulated Calcified Lesion? *Int Heart J* 2016;57(3):376-9.

40. Sugawara Y, Ueda T, Soeda T, Watanabe M, Okura H, Saito Y. Plaque modification of severely calcified coronary lesions by scoring balloon angioplasty using Lacrosse non-slip element: insights from an optical coherence tomography evaluation. *Cardiovasc Interv Ther* 2019;34(3):242-8.
41. Kurata N, Ishihara T, Iida O, et al. Predictors for Calcium Fracture With a Novel Cutting Balloon: An Optical Coherence Tomography Study. *JACC Cardiovasc Interv* 2022;15(8):904-6.